

Thermoluminescence under an exponential heating function: I. Theory

G Kitis¹, R Chen², V Pagonis³, E Carinou⁴ and V Kamenopoulou⁴

¹ Aristotle University of Thessaloniki, Nuclear Physics Laboratory, 54124-Thessaloniki, Greece

² School of Physics and Astronomy, Raymond and Beverly Sackler Faculty of Exact Sciences, Tel-Aviv University, Tel-Aviv 69978, Israel

³ Physics Department, McDaniel College, Westminster, MD 21157, USA

⁴ Greek Atomic Energy Commission, PO Box 60092, Ag. Paraskevi 15310, Greece

E-mail: gkitis@auth.gr

Received 30 November 2005, in final form 1 December 2005

Published 30 March 2006

Online at stacks.iop.org/JPhysD/39/1500

Abstract

Constant temperature hot gas readers are widely employed in thermoluminescence dosimetry. In such readers the sample is heated according to an exponential heating function. The single glow-peak shape derived under this heating condition is not described by the TL kinetics equation corresponding to a linear heating rate. In the present work TL kinetics expressions, for first and general order kinetics, describing single glow-peak shapes under an exponential heating function are derived. All expressions were modified from their original form of $I(n_0, E, s, b, T)$ into $I(I_m, E, T_m, b, T)$ in order to become more efficient for glow-curve deconvolution analysis. The efficiency of all algorithms was extensively tested using synthetic glow-peaks.

(Some figures in this article are in colour only in the electronic version)

1. Introduction

Constant temperature hot gas readers are widely employed in thermoluminescence dosimetry (TLD) and over the years have shown excellent performance. In these readers the gas flow is always present and the temperature of the gas is kept strictly constant. This keeps the conditions in the heating chamber very stable and consequently makes the heating of the sample very reproducible [1]. As the sample is inserted in a high temperature environment, it is heated according to an exponential heating function (EHF) [2]. The glow-curve obtained is characterized by a relatively poor resolution of the individual glow-peaks making the glow-curve deconvolution (GCD) procedure a difficult task [3].

The application of GCD analysis to TLD leads to significant improvements in dosimetric techniques. The dosimetric data in conventional TL readers are usually taken as the integrated area under a glow-curve, whereas in the case of hot gas readers, the total amount of light emitted during readout is taken to represent the dosimetric data. However, this method requires in most cases the application of complicated heat treatments in order to erase the TL signal in the low

temperature part of the dosimetric area. In all cases the TL signal in the temperature region above the dosimetric area cannot be used and its removal is a difficult task. All of these practical problems are automatically removed by applying a GCD analysis to the data. A deconvoluted glow-curve is highly informative. For example, the analysis of the individual glow-peaks in the glow-curve gives (a) their trapping parameters E and s , contributing thus to our basic understanding of the TL mechanism in TL detectors, (b) the exact integral of each glow-peak can be used to represent the dosimetric data and to improve the accuracy of the dose evaluation and (c) the background signal can be analysed accurately and the dosimetric TL signal can be determined even in the case of very low doses.

A single glow-peak algorithm is the basic unit for the GCD analysis procedure. Such single glow-peak algorithms exist for linear heating rates [4] but not for an EHF. Previous efforts to analyse the glow-curve obtained by constant temperature hot gas readers [1, 3] are not based on single glow-peak models corresponding to an EHF. Recently Kumar *et al* [5] used an EHF model to fit the glow-curve of CaSO_4 . Lawless and Lo [6] derived single glow-peak expressions for a variety of

non-linear heating applied to the glow-curves resulting from laser heating of the samples.

The aim of the present work is to derive single glow-peak algorithms for the first and general order kinetics, which describe experimental glow-peaks received by stable temperature hot gas readers in which the sample is heated according to an EHF [7].

2. TL kinetics with an EHF

Chen and Kirsh [2] (and references therein) review TL kinetics under non-linear heating rates. Among them is the case of an EHF, first proposed by Osada [8] and used by Dijk and Julius [1], for the case of the stable temperature hot gas TL readers in the form

$$T(t) = T_g - (T_g - T_0)e^{-\alpha t}, \quad (1)$$

where T_g is the hot gas temperature approached asymptotically with time, T_0 is the temperature at $t = 0$, with α in s^{-1} given by the expression

$$\alpha = \frac{\delta A}{m c_p}, \quad (2)$$

where δ is the heat transfer efficiency, A is the heated area, m the mass of the sample and c_p the heat capacity.

This heating scheme described above is the one we get 'naturally' if we let a cold sample warm up while being in thermal contact with an infinite thermal bath at temperature T_g . This situation exists in the stable temperature hot gas TL readers, where the 'cold' TL chip at room temperature is inserted in the readout chamber, which is at the much higher temperature, T_g , of the hot gas.

The heating rate β will be

$$\beta = \frac{dT}{dt} = \alpha(T_g - T). \quad (3)$$

Figure 1 shows an example of the temperature profile according to the EHF (equation (1)) and the respective heating rate given by equation (3). The heating starts with the highest heating rate and tends to zero when the temperature becomes equal to the gas temperature T_g . A TL with zero heating rate is equivalent to a prompt isothermal decay (PID).

Using equation (3), the first order kinetics equation [10], after elementary algebra, will become

$$I(T) = n_0 s \exp\left(-\frac{E}{kT}\right) \exp\left(-\frac{s}{\alpha} \int_{T_0}^T \frac{\exp(-E/kT')}{T_g - T'} dT'\right). \quad (4)$$

The general order equation is derived in a similar manner

$$I(T) = n_0 s'' \exp\left(-\frac{E}{kT}\right) \left[1 + \frac{(b-1)s''}{\alpha} \times \int_{T_0}^T \frac{\exp(-E/kT')}{T_g - T'} dT'\right]^{-b/(b-1)}, \quad (5)$$

with $s'' = s' n_0^{(b-1)}$.

The second order is obtained by equation (5) by setting $b = 2$, with $s' = s/N$.

For the sake of simplicity, in the following, it is convenient to use the parameter $s = s' n_0^{b-1}$, having units of s^{-1} .

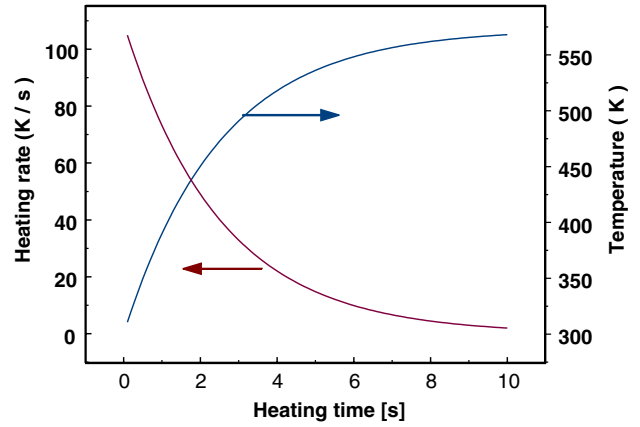


Figure 1. Temperature profile of an EHF according to equation (1) and the respective heating rate according to equation (3). $T_g = 573$ K and $\alpha = 0.4$ s^{-1} .

All the above derived expressions for the TL intensity $I(T)$ involve the integral

$$F(T, T_g, E) = \int_0^T \frac{\exp(-E/kT')}{T_g - T'} dT'. \quad (6)$$

Replacing $1/T'$ with x , E/k with p and T_g with α the exponential integral of equation (6) becomes an integral of the form

$$-\int_{\infty}^u \frac{e^{-px}}{x(ax-1)} dx = \int_{x=u}^{\infty} \frac{e^{-px}}{x(ax-1)} dx = -\int_u^{\infty} \frac{e^{-px}}{x} dx - \int_u^{\infty} \frac{e^{-px}}{((1/\alpha) - x)} dx. \quad (7)$$

Concerning the limits of integration the limit 0 becomes ∞ , whereas the limit T goes to $(1/T) = x$.

The second term of the right-hand side of equation (7) is of the following form, given by Gradshteyn and Ryzhik [11], which for $p > 0$ and $c < u$ is

$$\int_u^{\infty} \frac{e^{-px}}{c-x} dx = e^{-pc} Ei(pc - pu), \quad (8)$$

where $Ei(-u)$ is the exponential integral defined by [10, 11]

$$E_1(u) = -Ei(-u) = \int_u^{\infty} \frac{e^{-x}}{x} dx. \quad (9)$$

According to equation (8) the right-hand side of equation (7) becomes

$$-\int_u^{\infty} \frac{e^{-px}}{x} dx - \int_u^{\infty} \frac{e^{-px}}{((1/\alpha) - x)} dx = Ei(-px) - e^{-p/\alpha} Ei\left(\frac{p}{\alpha} - px\right). \quad (10)$$

Replacing x with $1/T$, p with E/k and α with T_g , the solution of the integral in equation (6) is obtained i.e.

$$F(T, T_g, E) = -\exp\left(-\frac{E}{kT_g}\right) Ei\left(\frac{E}{kT_g} - \frac{E}{kT}\right) + Ei\left(-\frac{E}{kT}\right). \quad (11)$$

Thus, the exponential integral of equation (6) can be written as

$$\int_{T_0}^T \frac{\exp(-E/kT')}{T_g - T'} dT' = F(T, T_g, E) - F(T_0, T_g, E). \quad (12)$$

For the case of linear heating function the respective exponential integral is [9]

$$\int_{T_0}^T \exp\left(-\frac{E}{kT'}\right) dT' = F(T, E) - F(T_0, E). \quad (13)$$

As shown by Chen [9], the values of the exponential integral at T_0 , $F(T_0, E)$ are negligible relative to the values $F(T, E)$ at some higher temperature T , since $F(T, E)$ is a very fast increasing function of T . Using the first two terms in the appropriate asymptotic series approximation (ASA) for the exponential integral (see equation (26)) and following the procedure of Chen [9], according to equation (11) we have

$$\begin{aligned} F(T, T_g, E) &\simeq -\exp\left(-\frac{E}{kT_g}\right) \exp\left(\frac{E}{kT_g} - \frac{E}{kT}\right) \\ &\times \frac{KT T_g}{E(T - T_g)} - \frac{kT}{E} \exp\left(-\frac{E}{kT}\right) \\ &\simeq -\frac{kT^2}{E} \frac{1}{T - T_g} \exp\left(\frac{E}{kT} \left(1 - \frac{T}{T_g}\right)\right). \end{aligned} \quad (14)$$

After some algebra one can obtain

$$\frac{F(T_0, T_g, E)}{F(T, T_g, E)} \simeq \frac{T_0^2}{T^2} \frac{T - T_g}{T_0 - T_g} \exp\left(\frac{E}{kT} \left(1 - \frac{T}{T_0}\right)\right). \quad (15)$$

The respective ratio for the case of linear heating rate given by Chen [9] is

$$\frac{F(T_0, E)}{F(T, E)} \simeq \frac{T_0^2}{T^2} \exp\left(\frac{E}{kT} \left(1 - \frac{T}{T_0}\right)\right). \quad (16)$$

Comparing equations (15) and (16) it is clear that the expression in equation (15) decreases with T faster than the expression in equation (16) by the factor $(T - T_g)/(T_0 - T_g)$.

Figure 2 shows the behaviour of equations (15) (curve (a)) and (16) (curve(b)) for the two extreme values of the activation energy E , where one can see that the term $F(T_0, T_g, E)$, indeed, becomes negligible very fast with increasing T and so can be ignored. Therefore, the following approximation of equation (12) can be considered a very good one for values of T not too close to T_0 .

$$\int_{T_0}^T \frac{\exp(-E/kT')}{T_g - T'} dT' \cong F(T, T_g, E). \quad (17)$$

The conditions at the maximum for the first and general order kinetics are evaluated by the condition

$$\frac{d \ln(I(T))}{dT} = 0. \quad (18)$$

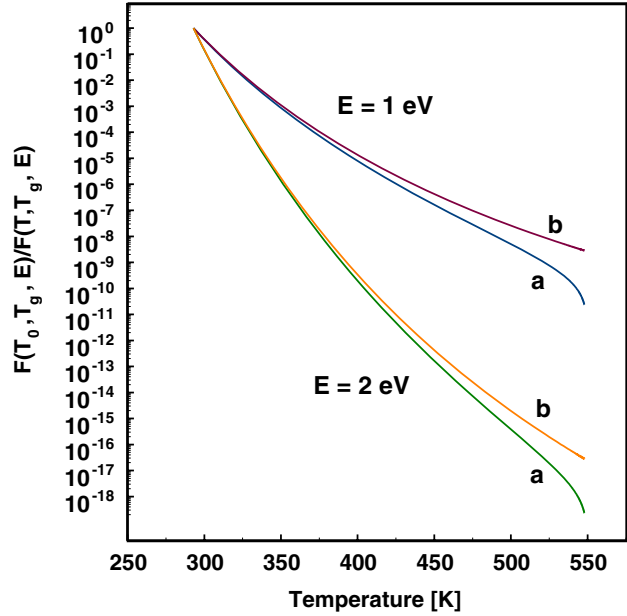


Figure 2. Behaviour of equation (15), curve(a), and equation (16), curve (b), for $E = 1$ and $E = 2$ eV.

The conditions at the maximum obtained for equations (4) and (5) are

$$\frac{\alpha E(T_g - T_m)}{kT_m^2} = s e^{-E/kT_m}, \quad (19)$$

$$\frac{\alpha(T_g - T_m)E}{bkT_m^2} \left(1 + \frac{(b-1)s}{\alpha} F(T_m, T_g, E)\right) = s'' e^{-E/kT_m}, \quad (20)$$

where $F(T_m, T_g, E)$ is the value of $F(T, T_g, E)$ at the temperature of the maximum TL intensity, T_m .

Normally, the expressions giving the TL intensity are of the form $I(n_0, E, s, T)$. However, in many practical situations, such as the GCD expressions of the form $I(I_m, T_m, E, T)$ are highly desirable. The reason is that the peak maximum intensity and temperature I_m, T_m , respectively, can be directly and accurately evaluated for the experimental glow-curve, whereas the values of n_0 and s are unknown. The $I(n_0, E, s, T) \rightarrow I(I_m, T_m, E, T)$ transformation procedure is described below.

The first order kinetics expression equation (4) becomes

$$I(T) = n_0 s \exp\left(-\frac{E}{kT}\right) \exp\left(-\frac{s}{\alpha} F(T, T_g, E)\right). \quad (21)$$

By substituting the value of s obtained from equation (19), into equation (21) the latter becomes

$$\begin{aligned} I(T) &= n_0 \frac{\alpha E(T_g - T)}{kT_m^2} \exp\left(-\frac{E(T_m - T)}{kT T_m}\right) \\ &\times \exp\left(-\frac{E(T_g - T)}{kT_m^2} \exp\left(\frac{E}{kT_m}\right) F(T, T_g, E)\right). \end{aligned} \quad (22)$$

Taking the value I_m of $I(T)$ at T_m and after some algebra one obtains

$$\begin{aligned} &n_0 \frac{\alpha E(T_g - T)}{kT_m^2} \\ &= I_m \exp\left(\frac{E(T_g - T)}{kT_m^2} \exp\left(\frac{E}{kT_m}\right) F(T_m, T_g, E)\right). \end{aligned} \quad (23)$$

Inserting the right-hand side of equation (23) into equation (22) the following is obtained:

$$I(T) = I_m \exp\left(-\frac{E(T_m - T)}{kTT_m} + \frac{E(T_g - T)}{kT_m^2}\right) \times \exp\left(\frac{E}{kT_m}\right) (F(T_m, T_g, E) - F(T, T_g, E)). \quad (24)$$

In a similar manner the respective expression for the general order case is obtained.

$$I(T) = I_m \exp\left(-\frac{E(T_m - T)}{kTT_m}\right) \times \left(1 - \frac{(b-1)(T_g - T_m)E}{bkT_m^2}\right) \exp\left(\frac{E}{kT_m}\right) \times (F(T_m, T_g, E) - F(T, T_g, E))^{-b/(b-1)}. \quad (25)$$

Equations (24) and (25) represent single glow-peak expressions, which depend on the experimental parameters I_m and T_m and not on n_0 and s . They will be ready for use by evaluating the appropriate values of $F(T, T_g, E)$, i.e. the values of the exponential integrals appearing in both the terms of equation (11). This can be achieved by two methods. The first method consists of a numerical evaluation of the exponential integrals in $F(T, T_g, E)$. This method was followed by Dijk and Julius [1]. This method is also followed in some modern software packages such as Mathematica, where the exponential integral is treated as a built-in like function. However, the most practical, flexible and software independent method is to obtain an analytical expression for a single glow-peak by replacing the term $F(T, T_g, E)$ by an appropriate approximation for the exponential integral.

The appropriate approximation depends upon the values of the argument z of the exponential integral $Ei[z]$. The function $F(T, T_g, E)$ given by equation (11) consists of two terms. In the case of the second term $Ei[-E/kT]$ the values of the argument $z = E/kT$ are, in all practical cases, always greater than 15 (i.e. $E > 15kT$). In this case the exponential integral can be approximated by the asymptotic series [9, 10], which for $z > 0$ is given by

$$-Ei(-z) = e^{-z} \sum_{n=0}^N \frac{(-1)^n n!}{z^{n+1}}. \quad (26)$$

It is of interest in the present work to discuss the accuracy of the ASA, which approximates the exponential integral in the region of arguments z relevant to the hot gas readers. The question is how many terms are needed for the most accurate approximation. According to Chen [9, 10], the number of terms N of the ASA to be taken is the largest integer smaller than z (in absolute value). For example, $z = 10$, one should take 10 terms. The error is minimized by adding one half of the next term with the appropriate sign. Therefore, the second term $Ei[-E/kT]$ of equation (11) is always very well approximated by the ASA of equation (26) by following the above described rule of Chen [9, 10].

The situation is different with the first term of $F(T, T_g, E)$, in equation (11), with argument $z = (E/kT_g) - (E/kT)$. Figure 3 shows the values of z in a temperature region typical of glow-curves received by a stable temperature hot gas reader. Practically, as seen in figure 3, the major part of such glow-curves should be characterized by arguments z between 10

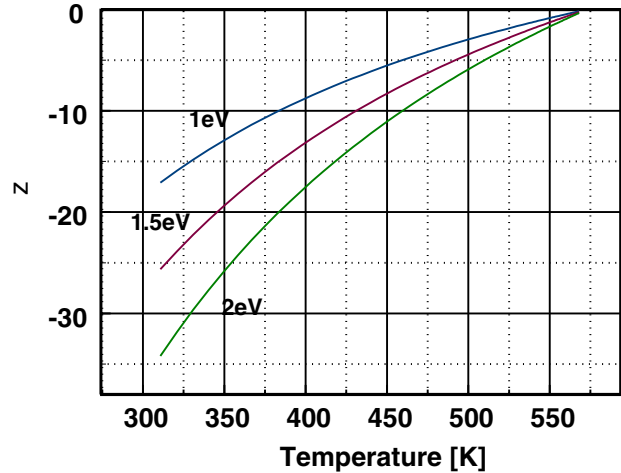


Figure 3. The argument $z = (E/kT_g) - (E/kT)$ of the exponential integral appearing in the first term of equation (11) as a function of temperature for three values of activation energy.

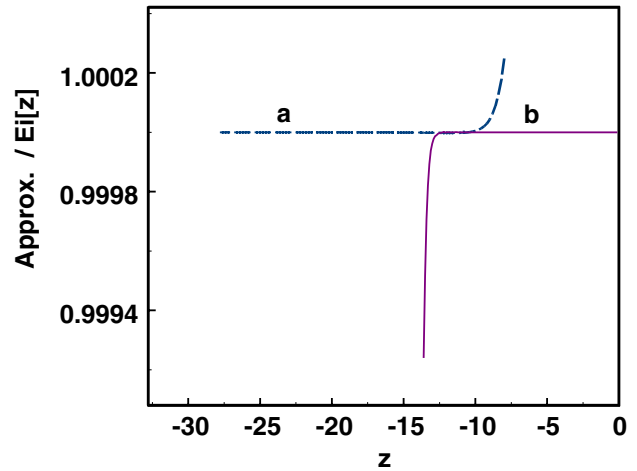


Figure 4. Approximation to the exponential integral used in the present work. (a) ASA with 10 terms plus one half of the 11th term, (b) CSA with 50 terms.

and 0. However, the accuracy of ASA drops substantially as z approaches 0. So instead of ASA, in the range of z (10, 0), the integral can be evaluated by another very well-known approximation of the exponential integral, the convergent series approximation (CSA) [10], which, for $z > 0$, is given by

$$Ei(-z) = \gamma + \ln(z) + \sum_{n=1}^{\infty} \frac{(-z)^n}{n \cdot n!}, \quad (27)$$

where $\gamma = 0.577 215 664 9$ is the Euler constant.

The question is how many terms are needed in order to have an accurate approximation in the whole region of $|z|$ between 10 and 0. It is found that using 50 terms of the CSA, the exponential integral is very accurately approximated up to $|z| = 10$, as shown in figure 4(b). Curve (a) in figure 4 shows the ASA approximation with $N = 10$. The argument value of $|z| = 10$ is a limit, which leads to the following suggestion. For z greater than 10 the ASA approximation must be used with the accuracy being kept at the sixth significant figure by increasing appropriately the number of terms in equation (26)

and for $|z|$ between 10 and 0 the CSA must be used with the accuracy being kept at the sixth significant figure by decreasing the number of terms in equation (27).

3. Analytical single glow-peak algorithms

Analytical single glow-peak kinetic equation of the first and general order of kinetics of the form $I(n_0, E, s, T)$ and $I(n_0, E, s, b, T)$ can be derived by substituting the above-described exponential integral approximations to the general expression given by equations (4) and (5).

The next step is to use the general form given by equations (24) and (25) and the appropriate approximation for the $F(T, T_g, E)$ in order to transform the $I(n_0, E, s, T)$ and $I(n_0, E, s, b, T)$ equations into equations of the forms $I(I_m, E, T_m, T)$ and $I(I_m, E, T_m, b, T)$, respectively, which are much more efficient and easily implemented for GCD.

3.1. Asymptotic series approximation

Using the ASA for both the terms of $F(T, T_g, E)$ in equation (11) the first and general order kinetics equations, $I(n_0, E, s, T)$ and $I(n_0, E, s'', b, T)$, for an EHF glow-peak are

$$I(T) = n_0 s \exp\left(-\frac{E}{kT}\right) \exp\left[-\frac{skT}{\alpha E} \exp\left(-\frac{E}{kT}\right) Z(T)\right], \quad (28)$$

$$I(T) = n_0 s'' \exp\left(-\frac{E}{kT}\right) \times \left[1 + \frac{(b-1)s''kT}{\alpha E} \exp\left(-\frac{E}{kT}\right) Z(T)\right]^{-b/(b-1)}, \quad (29)$$

where

$$Z(T) = \sum_{n=0}^N (-1)^n n! D^n (B^{n+1} - 1) + EC, \quad (30)$$

$$B = \frac{T_g}{T_g - T}, \quad (31)$$

$$D = \frac{kT}{E}. \quad (32)$$

where $E \cdot C$ is an error correction term which has to be taken into account when ASA, (equation (30)), is used [9, 10] (see also the discussion on equation (30)). However, in this case special care must be taken about the number N of terms in equation (30), since it is a combination of two asymptotic series each having a different optimal value of N . Suppose, for example, that the arguments (in absolute value) of the terms $z = |(E/kT_g) - (E/kT)|$ and $z = |E/kT|$ in equation (11) are 10 and 20, respectively. Then the number of terms in equation (30) will be $N_1 = 10$ and $N_2 = 20$. In equation (30) taking $N = 20$ for the combination is not good because once the optimal number for the term with $z = 10$ is passed the error grows quite significantly. On the other hand taking $N = 10$ in equation (30), i.e. the optimal value for the first term but not for the second, the combination will be good because when the argument is that large (in absolute value) the approximation will be good even with a smaller number of terms, 10 in the present example. Note that the contribution of

the exponential integral with argument $z = |E/kT| = 10$ is much smaller than the contribution of the exponential integral with $z = |(E/kT_g) - (E/kT)| = 20$, so that the accuracy in the exponential integral with $z = |(E/kT_g) - (E/kT)| = 20$ is of major importance. In conclusion, the number of terms in equation (30) will be given by the value of the term $z = (E/kT_g) - (E/kT)$, which is represented in equation (30) by the term B .

The equivalent $I(I_m, E, T_m, T)$ equation for the first and $I(I_m, E, T_m, b, T)$ general order kinetics, which are obtained from equation (24) and equation (25), respectively, are

$$I(T) = I_m \exp\left[-\frac{E(T_m - T)}{kTT_m} + \frac{T_g - T_m}{T_m}\right] \times \left(Z_m - \frac{T}{T_m} \exp\left[-\frac{E(T_m - T)}{kTT_m}\right] Z(T)\right), \quad (33)$$

and

$$I(T) = I_m \exp\left[-\frac{E(T_m - T)}{kTT_m}\right] \left[1 - \frac{(b-1)T_g - T_m}{bT_m}\right] \times \left(Z_m - \frac{T}{T_m} \exp\left[-\frac{E(T_m - T)}{kTT_m}\right] Z(T)\right)^{-b/(b-1)}, \quad (34)$$

where Z_m is the value of $Z(T)$ at T_m .

The second order kinetics is obtained by setting $b = 2$.

3.2. Convergent series approximation

Using the CSA for the first term of the $F(T, T_g, E)$, (equation (11)) and the asymptotic series for the second term, the first $I(n_0, E, s, T)$ and general order kinetics equations, $I(n_0, E, s'', b, T)$, for an EHF glow-peak are

$$I(T) = n_0 s \exp\left(-\frac{E}{kT}\right) \exp\left[-\frac{s}{\alpha} \exp\left(-\frac{E}{kT_g}\right) Z_1(T)_{(CSA)} - \frac{kT}{E} Z_2(T) \exp\left(-\frac{E}{kT}\right)\right], \quad (35)$$

$$I(T) = n_0 s'' \exp\left(-\frac{E}{kT}\right) \times \left[1 + \frac{(b-1)s''}{\alpha} \exp\left(-\frac{E}{kT_g}\right) Z_1(T)_{(CSA)} - \frac{kT}{E} Z_2(T) \exp\left(-\frac{E}{kT}\right)\right]^{-b/(b-1)}, \quad (36)$$

where

$$Z_1(T)_{(CSA)} = \gamma + \ln |G(T)| + \sum_{n=1}^{50} \frac{G(T)^n}{n \cdot n!}, \quad (37)$$

$$Z_2(T) = \sum_{n=0}^N (-1)^n n! D^n + EC, \quad (38)$$

$$G(T) = \frac{E}{kT} \frac{T - T_g}{T_g}, \quad (39)$$

$$D = \frac{KT}{E}, \quad (40)$$

where EC is an error correction term which is equal to the one half of the $(N+1)^{\text{th}}$ term of equation (38), with the appropriate sign, which is added in order to minimize the error due to the use of a limited number of terms in ASA [9, 10] (see also the discussion on equation (30)).

The equivalent $I(I_m, E, T_m, T)$ equations for the first and $I(I_m, E, T_m, b, T)$ for the general order kinetics, which are obtained from equation (24) and equation (25), respectively, are

$$I(T) = I_m \exp \left[-\frac{E(T_m - T)}{kTT_m} - \frac{E(T_g - T_m)}{kT_m^2} \right] \times \exp \left(\frac{E(T_g - T_m)}{kT_m T_g} \right) \times (Z_1(T_m) - Z_1(T))_{(CSA)} - \frac{T_g - T_m}{T_m} \times \left(Z_2(T_m) - Z_2(T) \frac{T}{T_m} \exp \left(-\frac{E(T_m - T)}{kTT_m} \right) \right) \quad (41)$$

and

$$I(T) = I_m \exp \left(-\frac{E(T_m - T)}{kTT_m} \right) \times \left[1 - \frac{(b-1)(T_g - T_m)}{bT_m} \left(\frac{E}{kT_m} \exp \left(\frac{E(T_g - T_m)}{kT_g T_m} \right) \right) \times (Z_1(T) - Z_1(T_m))_{(CSA)} + \frac{T}{T_m} Z_2(T) \times \exp \left(-\frac{E(T_m - T)}{kTT_m} \right) - Z_2(T_m) \right]^{b/(b-1)}, \quad (42)$$

where $Z_1(T_m)$ and $Z_2(T_m)$ the values of $Z_1(T)$ and $Z_2(T)$ at T_m .

4. Simulations of glow-peaks under EXF

The analytical expressions derived in the present work should be tested with synthetic glow-peaks evaluated without the need to approximate the exponential integral. Such synthetic glow-peaks called reference glow-peaks (RGP) can be produced by software packages in which the exponential integral is very accurately evaluated by numerical integration, for example, Mathematica. The parameters used for the evaluation of RGP are $E = 1 \text{ eV}$, $s = 10^{12} \text{ s}^{-1}$, $n_0 = 10^{13} \text{ cm}^{-3}$. The parameter α of the EHF was taken equal to 0.1 s^{-1} and $T_0 = 293 \text{ K}$. By keeping the listed parameters constant, RGPs were simulated as a function of T_g , i.e. the temperature of the hot gas. Simultaneously, the first order kinetics glow-peaks were simulated using the analytical glow-peak expressions given by equations (28) and (35).

The curve fitting procedure is performed using the MINUIT program [12] and goodness of fit was tested using the figure of merit (FOM) introduced by Balian and Eddy [13] given by

$$\text{FOM} = \sum_i \frac{|Y_{\text{Exper}} - Y_{\text{Fit}}|}{A}, \quad (43)$$

where Y_{Exper} is the experimental glow-curve, Y_{fit} is the fitted glow-curve and A is the area of the fitted glow-curve.

4.1. Tests of the $I(I_m, E, T_m, T)$ algorithms

The GCD analysis of complex TL glow-curves can be performed using equations (28), (35), (29) and (36). In these equations the free parameters are the n_0 , E , s and b . Moreover, the parameter α of the EHF is usually not known. Therefore, single glow-peak algorithms, which will

Table 1. Tests of algorithms derived assuming both ASA and CSA for the exponential integral.

T_{gas} (K)	FOM	E	s
Fit of $I(I_m, E, T_m, T)$ (equation (33)) to RGP			
500	7.6×10^{-2}	0.975	3.9×10^{11}
550	1.8×10^{-2}	0.979	5.3×10^{11}
600	4.5×10^{-3}	0.995	8.4×10^{11}
650	4.7×10^{-4}	1.0	1.0×10^{12}
700	2.1×10^{-4}	1.0	1.0×10^{12}
Fit of CSA $I(I_m, E, T_m, T)$ (equation (41)) to RGP			
360	1.8×10^{-5}	1.0	1.0×10^{12}
380	1.6×10^{-5}	1.0	1.0×10^{12}
400	3.5×10^{-6}	1.0	1.0×10^{12}
420	4.7×10^{-6}	1.0	1.0×10^{12}
460	2.1×10^{-5}	1.0	1.0×10^{12}
480	1.0×10^{-4}	1.0	1.0×10^{12}
500	7.8×10^{-4}	1.0	1.0×10^{12}
520	1.2×10^{-3}	1.0	1.0×10^{12}
550	9.6×10^{-3}	1.0	9.5×10^{11}
600	1.4×10^{-2}	1.0	7.2×10^{11}
Fit of ASA plus PSA $I(I_m, E, T_m, T)$ to RGP			
480	7.7×10^{-5}	1.0	1.0×10^{12}
500	3.5×10^{-5}	1.0	1.0×10^{12}
520	1.8×10^{-5}	1.0	1.0×10^{12}
550	4.1×10^{-6}	1.0	1.0×10^{12}
600	3.2×10^{-5}	1.0	1.0×10^{11}

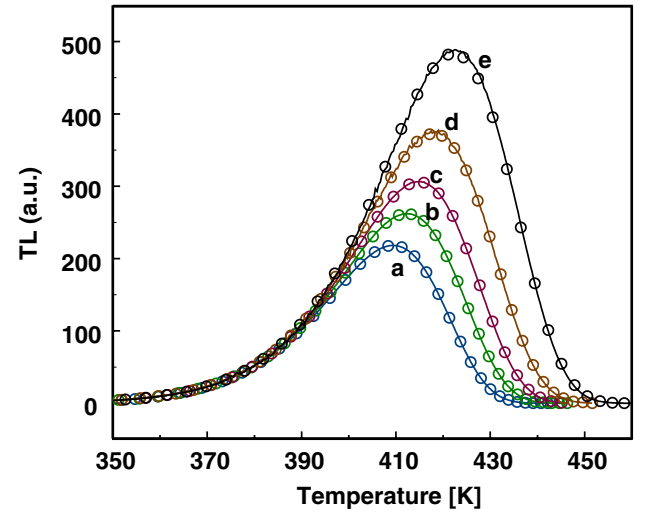


Figure 5. Fit of the first order RGP, (O) with the CSA expression given by equation (41) (—) for various gas temperatures T_g (a) 480 K, (b) 500 K, (c) 520 K, (d) 550 K and (e) 600 K.

be dependent on experimentally obtainable parameters, such as I_m and T_m and independent of α , are highly desirable. These kinds of algorithms derived in the present work are based on equations (33), (34), (41) and (42).

The newly obtained algorithms have to pass a double test. The first test is to examine how successful the $I(n_0, E, s'', b, T) \rightarrow I(I_m, E, T_m, b, T)$ transformation is for $b = 1$ and 2. The test was applied to all algorithms, of the first and general order kinetics, derived. The goodness of fit was tested by FOM defined above. The FOM values obtained were in all the cases between 9×10^{-6} – 8×10^{-7} . These values mean that the algorithms of the form $I(n_0, E, s'', b, T)$, in fact, coincide numerically with their respective $I(I_m, E, T_m, b, T)$ form.

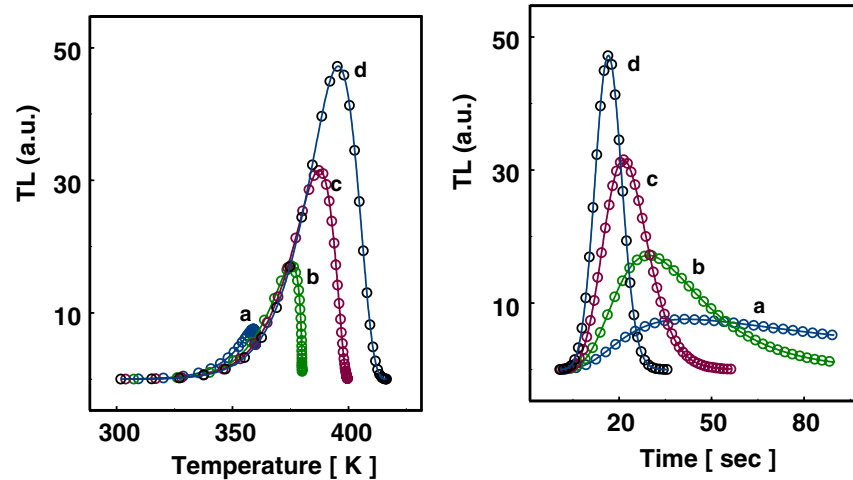


Figure 6. Fit of the first order RGP (○) with the CSA expression given by equation (41) (—) for various gas temperatures T_g (a) 360 K, (b) 380 K, (c) 400 K and (d) 420 K. The figure on the right-hand side shows the same data as the figure on the left-hand side on a time-scale instead of a temperature scale.

The second test is to find the degree to which the first order kinetics $I(I_m, E, T_m, T)$ algorithm fits the RGP directly. The fitting of the RGP with the ASA $I(I_m, T_m, E, T)$ algorithm given by equation (33) is very good. The FOM, E and s values obtained are listed in table 1. As is seen the FOM values are highly improved as the T_g temperature increases. The reason is that at low T_g temperatures, for a part of the glow-peak, the argument z of the exponential integral is less than 10, where the accuracy of ASA is not sufficient. However, as the T_g increases the argument, z , of the exponential integral is shifted to values greater than 10, where the ASA is very accurate as shown in figure 4(a).

The fitting of the RGP by the first order kinetics CSA $I(I_m, T_m, E, T)$ algorithm, given by equation (41), is very successful as shown by the FOM values obtained and listed in table 1. The very good FOM values at low T_g are due to the fact that the argument z of the exponential integral is exactly within region (10,0), where the CSA approximates the exponential integral very accurately. However, as seen from table 1, as the T_g increases the FOM values are increased, which means that the fitting becomes worse. The reason is, as discussed in the previous paragraph, that as the T_g increases the argument z of the exponential integral becomes greater than 10 where only the ASA holds.

From the above two series of fitting it becomes clear that there exist glow-peaks for which (see also figure 4) one part of the glow-peak requires use of the ASA of the exponential integral, whereas the other part requires a CSA of the exponential integral. For these cases a fitting function can be used, which takes the values of the ASA when the argument z of the exponential integral is greater than 10 and it takes the values of CSA when the argument z is between 10 and 0. Examples of such fitting are listed in the last part of table 1, where one can see that the FOM values obtained are significantly improved.

Examples of the glow-curve shapes calculated under EHF are shown in figure 5. The open circles correspond to the RGP and the solid lines to the fitting using the CSA approximation (equation (41)), as a function of T_g . As the T_g increases, the heating rate increases according to equation (3), so that

the behaviour of the glow-peaks in figure 5 is similar to the behavior of the glow-peaks obtained with a linear heating function (see, e.g. [10, pp 30,32]).

The CSA shows its capabilities when T_g is set to a temperature, which is just below the peak maximum temperature of a glow-peak. In such a case, the part of the glow-peak up to T_g is a normal readout, whereas as the temperature approaches asymptotically T_g , the TL seems to decay under isothermal conditions and it is very similar to the PID readout. Examples of such glow-peaks are shown in figure 6. The left-hand side figure 6 shows the simulated RGPs (open circles) in a temperature scale, fitted by equation (41) represented by solid lines. Let us take as an example the curve (a), for which the FOM is 1.8×10^{-5} . Initially the temperature rises rapidly and a rising part of the glow-peak is obtained. However, when the temperature gets very close to temperature $T_g = 360$ K, the TL simply decays at an almost constant temperature, so that the TL seems to be accumulated at the same point. However, if curve (a) on the left-hand side of figure 6 is plotted as a function of time then curve (a) on the right-side of figure 6 is obtained, where one can see a very good fit. Curves (b)–(d) show the same effects as curve (a) at a higher temperature T_g .

5. Conclusions

Thermoluminescence kinetics equations of the first and general order kinetics describing glow-peaks received under an EHF are derived. The derived equations of the forms $I(n_0, E, s, T)$ and $I(n_0, E, s'', b, T)$ were transformed into $I(I_m, E, T_m, T)$ and $I(I_m, E, T_m, b, T)$. The latter depends on parameters I_m and T_m instead of n_0 and s , which are directly obtained from the experimental glow-peaks thus making the derived single glow-peak equation more effective for the computerized GCD.

The newly obtained equations of the form $I(I_m, E, T_m, T)$ were successfully tested using synthetic RGP obtained for a variety of exponential heating conditions.

References

- [1] Dijk Van J W E and Julius H W 1993 *Radiat. Prot. Dosim.* **47** 479
- [2] Chen R and Kirsh Y 1981 *Analysis of Thermally Stimulated Processes* (Oxford: Pergamon) p 167
- [3] Gomez Ros J M, Muniz J L, Delgado A, Bøtter-Jensen L and Jorgensen F 1993 *Radiat. Prot. Dosim.* **47** 483
- [4] Kitis G, Gomez Ros J M and Tuyn J W N 1998 *J. Phys. D: Appl. Phys.* **31** 2636
- [5] Kumar M, Alagu Raja E, Prasad L C, Kher P K and Bhatt B C 2005 *Radiat. Prot. Dosim.* **113** 366
- [6] Lawless J L and Lo D 2001 *J. Applied Phys.* **89** 6145
- [7] Kitis G, Chen R, Pagonis V, Carinou E, Ascounis P and Kamenopoulou V 2006 *J Phys D: Appl. Phys.* **39** 1508 (Part II, following paper)
- [8] Osada K 1960 *J. Phys. Soc. Japan* **15** 145
- [9] Chen R 1969 *J. Comput. Phys.* **4** 415
- [10] Chen R and McKeever S W S 1997 *Theory of Thermoluminescence and Related Phenomena* (Singapore: World Scientific) p 262
- [11] Gradshteyn I S and Ryzhik I M 1980 *Tables of Integrals, Series and Products* (New York: Academic) p 311
- [12] James F and Roos M 1977 *MINUIT* CERN Program Library Entry D506 <http://consult.cern.ch/writeups/minuit>
- [13] Balian H G and Eddy N W 1977 *Nucl. Instrum. Methods* **145** 389